Genomics **61,** 243–258 (1999)
Article ID geno.1999.5976, available online at http://www.idealibrary.com on IDEAL®

Characterization of the Human and Mouse Unconventional Myosin XV Genes Responsible for Hereditary Deafness *DFNB3* and Shaker 2

Yong Liang,*,†,[1] Aihui Wang,*,†,[1] Inna A. Belyantseva,‡ David W. Anderson,* Frank J. Probst,§ Thomas D. Barber,*,† Webb Miller,¶ Jeffrey W. Touchman,‖ Long Jin,** Susan L. Sullivan,†† James R. Sellers,‡‡ Sally A. Camper,¶ Ricardo V. Lloyd,** Bechara Kachar,‡ Thomas B. Friedman,* and Robert A. Fridell*,[2]

*Laboratory of Molecular Genetics, National Institute on Deafness and Other Communication Disorders (NIDCD), National Institutes of Health (NIH), 5 Research Court, Rockville, Maryland 20850; †Graduate Program in Genetics, Michigan State University, East Lansing, Michigan 48824; ‡Laboratory of Cellular Biology, NIDCD, NIH, Bethesda, Maryland 20892; §Department of Human Genetics, University of Michigan, Ann Arbor, Michigan 48109; ¶Department of Computer Science and Engineering, Pennsylvania State University, University Park, Pennsylvania 16802; ‖NIH Intramural Sequencing Center, NIH, Gaithersburg, Maryland 20877; **Department of Laboratory Medicine and Pathology, Mayo Clinic, Rochester, Minnesota 55905; ††Laboratory of Molecular Biology, NIDCD, NIH, Rockville, Maryland 20850; and ‡‡Laboratory of Molecular Cardiology, National Heart, Lung and Blood Institute, NIH, Bethesda, Maryland 20892

Received July 1, 1999; accepted September 2, 1999

Mutations in myosin XV are responsible for congenital profound deafness *DFNB3* in humans and deafness and vestibular defects in shaker 2 mice. By combining direct cDNA analyses with a comparison of 95.2 kb of genomic DNA sequence from human chromosome 17p11.2 and 88.4 kb from the homologous region on mouse chromosome 11, we have determined the genomic and mRNA structures of the human (*MYO15*) and mouse (*Myo15*) myosin XV genes. Our results indicate that full-length myosin XV transcripts contain 66 exons, are >12 kb in length, and encode 365-kDa proteins that are unique among myosins in possessing very long ~1200-aa N-terminal extensions preceding their conserved motor domains. The tail regions of the myosin XV proteins contain two MyTH4 domains, two regions with similarity to the membrane attachment FERM domain, and a putative SH3 domain. Northern and dot blot analyses revealed that myosin XV is expressed in the pituitary gland in both humans and mice. Myosin XV transcripts were also observed by *in situ* hybridization within areas corresponding to the sensory epithelia of the cochlea and vestibular systems in the developing mouse inner ear. Immunostaining of adult mouse organ of Corti revealed that myosin XV protein is concentrated within the cuticular plate and stereocilia of cochlear sensory hair cells. These results indicate a likely role for myosin XV in the formation or maintenance of the unique actin-rich structures of inner ear sensory hair cells.

Sequence data from this article have been deposited with the GenBank Data Library under Accession Nos. AF144093, AF144094, AF144095, and AF051976.

[1] These authors contributed equally to this work.

[2] To whom correspondence should be addressed. Telephone: (301) 435-8110. Fax: (301) 480-8019. E-mail: fridellr@nidcd.nih.gov.

INTRODUCTION

Recessive congenital nonsyndromic deafness *DFNB3* was originally identified in a kindred in Bengkala, Bali and subsequently mapped to a 3-cM region on chromosome 17p11.2 within the Smith–Magenis syndrome critical region (Friedman *et al.*, 1995; Liang *et al.*, 1998). On the basis of conserved synteny, the mouse deafness locus shaker 2 (*sh2*) was proposed as a model for *DFNB3* (Liang *et al.*, 1998). This prediction was verified when mutations in the human and mouse unconventional myosin XV genes were shown to cause *DFNB3* and *sh2*, respectively (Probst *et al.*, 1998; Wang *et al.*, 1998). In humans, three different myosin XV (*MYO15*) mutations were found to cosegregate with profound congenital deafness in three unrelated families, two in India and one in Bali (Wang *et al.*, 1998). In *sh2* mice, a myosin XV (*Myo15*) mutation was identified, and the *sh2* phenotypes of circling, head tossing, and deafness were rescued by germline injection of a BAC clone containing the *Myo15* gene (Probst *et al.*, 1998).

Myosins are molecular motors that use energy from ATP hydrolysis to pull against or move along actin filaments. The myosin superfamily includes conventional class II myosins and 14 classes of unconventional myosins. Myosin family members share a structural organization consisting of a conserved head or motor domain, a neck region with myosin light chain-binding sites, and a divergent tail domain (Cope *et al.*, 1996; Mermall *et al.*, 1998; Mooseker and Cheney, 1995; Sellers, 1999). The filament forming class II my-

0888-7543/99 $30.00

osins of muscle and nonmuscle cells have been extensively studied and are relatively well characterized (Sellers, 1999). In contrast, an understanding of the mechanochemical and biological properties of many of the unconventional myosins is just beginning to emerge. Proposed functions for unconventional myosins include roles in organelle movement, membrane trafficking, and the subcellular localization of specific proteins or RNAs (Baker and Titus, 1998; Mermall *et al.,* 1998).

In addition to myosin XV, two other unconventional myosin genes are associated with hearing loss in humans and mice. The profound deafness and vestibular defects of Snell's waltzer and shaker 1 mice are caused by mutations in myosin VI (*Myo6*) and myosin VIIA (*Myo7a*), respectively (Avraham *et al.,* 1995; Mburu *et al.,* 1997). In humans, *MYO7A* mutations are associated with dominant (*DFNA11*) and recessive (*DFNB2*) nonsyndromic deafness, as well as with Usher syndrome type 1b, a recessive disorder characterized by congenital deafness and progressive retinal degeneration (Chen *et al.,* 1996; Liu *et al.,* 1997a,b; Weil *et al.,* 1995, 1996, 1997). Both Myo6 and Myo7a are present in sensory hair cells of the inner ear, but their roles in the auditory and vestibular systems remain unclear (Avraham *et al.,* 1997; Hasson *et al.,* 1995, 1997). Another unconventional myosin, myosin 1β (Myo1β), is found at the tip-link region of cochlear hair cell stereocilia and has been proposed to be a component of a motor complex that mechanically resets gated ion channels to maintain optimal sensitivity to physical sound stimuli (Garcia *et al.,* 1998; Gillespie *et al.,* 1993; Hasson *et al.,* 1997; Steyger *et al.,* 1998). Given the diversity and critical nature of unconventional myosins in sensory cells of the auditory system, further study of these motor proteins offers a unique opportunity to understand better the molecular mechanics underlying sound transduction.

We previously reported partial cDNA sequences of the human (4.8 kb) and mouse (5.35 kb) myosin XV genes (GenBank Accession Nos. AF051976 and AF053130; Probst *et al.,* 1998; Wang *et al.,* 1998). A partial *Myo15* cDNA (1.76 kb, GenBank Accession No. AB014510) was also independently described (Wakabayashi *et al.,* 1998). Here, we markedly extend these findings by providing complete genomic and cDNA structures of the human and mouse myosin XV genes. We also present a comparative analysis of approximately 95 kb of human and mouse genomic DNA sequences and report the results of myosin XV expression studies. These data will facilitate the identification of myosin XV mutations associated with deafness and also provide insight into the function of myosin XV in normal sound transduction.

MATERIALS AND METHODS

Sequencing and genomic DNA analysis. The sequence of a cosmid containing 39.5 kb of the human *MYO15* gene (155d02, GenBank Accession No. AF051976) has been reported (Wang *et al.,* 1998). Two additional cosmids (145g11 and 3h3) were isolated from an arrayed chromosome 17 library using PCR products from the ends of cosmid 155d02 as probes. The sequences of these cosmids were determined as described (Wilson and Mardis, 1997). Briefly, cosmid DNA was kinetically sheared, and random fragments were subcloned. Sequences of individual clones were obtained with dye terminator (PE Applied Biosystems, Norwalk, CT) and dye primer (Amersham-Pharmacia Biotech, Arlington Heights, IL) chemistries on ABI 377xl automated DNA sequencers. The complete sequence of the inserts of cosmids 145g11 (36.8 kb) and 3h3 (34.2 kb) were determined by assembling 982 and 582 random sequences, respectively, with the Phred/Phrap/Consed suite of programs (Ewing and Green, 1998; Ewing *et al.,* 1998; Gordon *et al.,* 1998). Error frequencies (estimated by the program Phrap) were 1.07 in 10^4 bp (145g11) and 0.78 in 10^4 bp (3h3). A 95.2-kb contig compiled from cosmids 155d02, 145g11, and 3h3 has been deposited with GenBank (Accession No. AF051976).

Using a similar approach, the ~140-kb insert from mouse strain 129/Sv of the BAC clone 425p24, containing the *Myo15* gene, was partially assembled from 1142 random shotgun DNA sequences. Together with the sequence of directed PCR products (used to fill small gaps between the assembled sequence contigs), an 88.4-kb sequence contig, containing the *Myo15* gene in its entirety, was constructed (GenBank Accession No. AF144093). DNA sequence assembly and editing was performed with the Sequencher program (Genecodes, Ann Arbor, MI).

The percent identity plot of the human and mouse genomic sequence contigs was prepared as follows. Interspersed repetitive elements were first masked with RepeatMasker (A.F.A. Smit and P. Green, http://ftp.genome.washington.edu/RM/RepeatMasker.html), and then the human and mouse sequences were aligned using an experimental version of the Blast program (Altschul *et al.,* 1997). A percent identity plot of that alignment was created with a program called "laps" (Schwartz *et al.,* 1991). Of 65 *MYO15* coding exons, all but the 6-bp exon 8 were readily predicted on the basis of conservation between the human and the mouse genomic sequences.

FIG. 1. (**A**) Comparative analysis of the human and mouse myosin XV genomic regions. The chromosomal positions of three overlapping human cosmid clones and mouse BAC clone 425p24 that contain myosin XV and most of an adjacent GTP-binding protein gene, *DRG2,* are represented. The vertical numbered lines indicate the starting positions of exons identified in human and mouse cDNA fragments. The positions of predicted translation start and termination signals are shown as are two polyadenylation signals identified in human *MYO15* EST clones. Use of the first polyadenylation signal would result in a MYO15 protein with 39 different residues replacing the C-terminal 79 amino acids of the full-length protein. The positions of *Alu* (human) and B-family SINE (mouse) interspersed repetitive elements are designated by triangles. Closed circles indicate the positions of six SNPs identified in *MYO15* coding exons (see Table 1). *D17S2206* and *D17S2207* are newly identified highly polymorphic dinucleotide repeats within the *MYO15* gene (see Table 1). (**B**) Percent identity plot of the human *MYO15* genomic region showing percentage of nucleotide identity in segments between consecutive gaps in an alignment with the homologous mouse sequence. Human exons identified in cDNA fragments are represented by dark rectangles and are numbered. The 3′ untranslated regions of the *MYO15* and *DRG2* genes are indicated by open rectangles. Interspersed repeats identified by RepeatMasker are drawn as: L1, white pointed box; MIR, black triangle; other SINE, light gray triangle; all other elements, dark gray. Low rectangles (e.g., around 92 k) identify CpG islands in the human sequence, with white indicating a CpG/GpC ratio >0.6 and dark gray for CpG/GpC >0.75. Identical matches to mouse (e.g., W62803) and human (e.g., D81994) EST clones were returned by BLAST searches with the conserved region, labeled mouse ESTs, around 92 kb. These EST clones are likely derived from an adjacent gene downstream of *MYO15.*

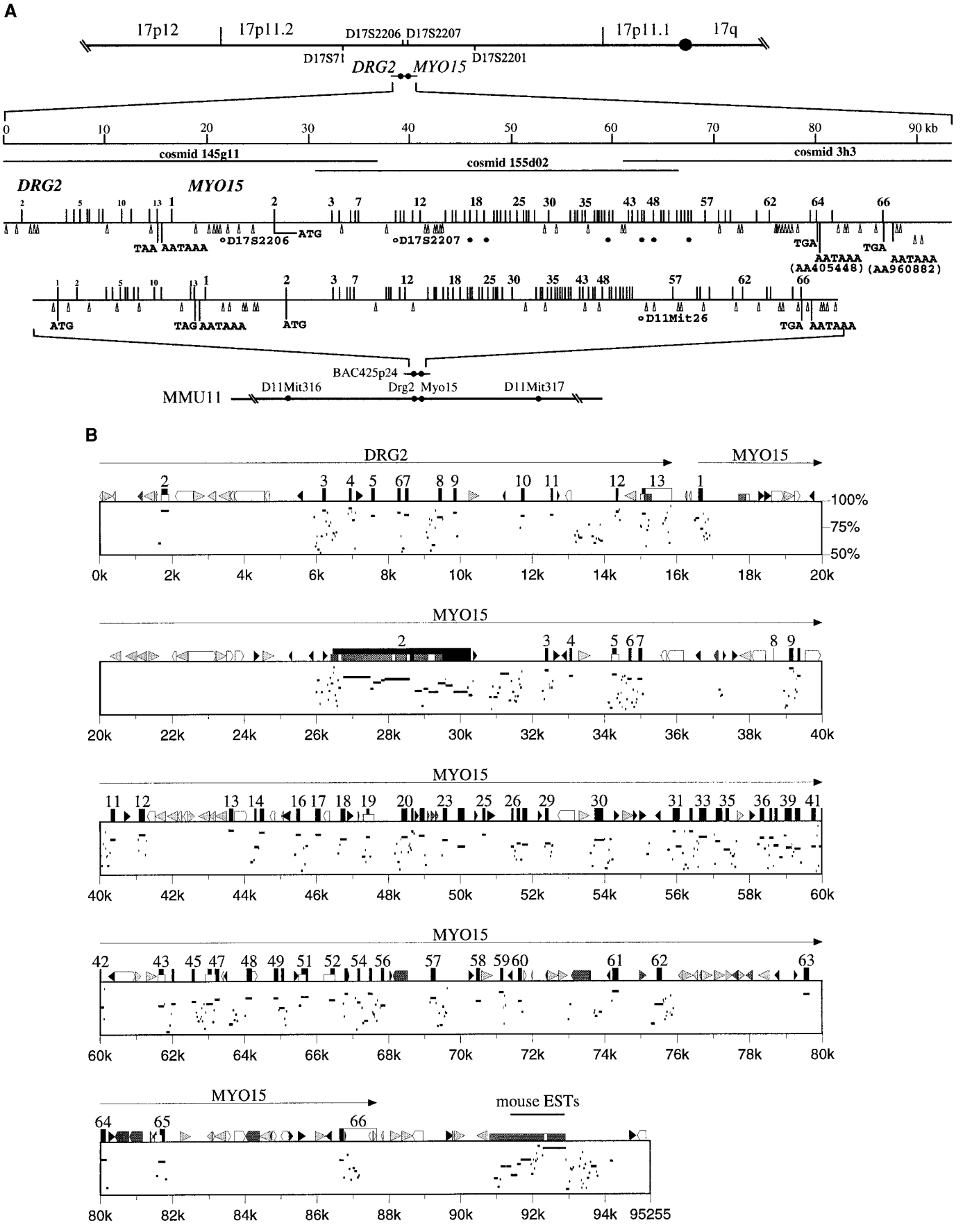
A
17p12
17p11.2
D17S2206 D17S2207
17p11.1
17q
D17S71
DRG2 MYO15
D17S2201
0 10 20 30 40 50 60 70 80 90 kb
cosmid 145g11
cosmid 155d02
cosmid 3h3
DRG2
MYO15
TAA AATAAA
D17S2206
ATG
D17S2207
TGA
AATAAA
(AA405448)
TGA
AATAAA
(AA960882)
ATG
TAG AATAAA
ATG
D11Mit26
TGA AATAAA
BAC425p24
MMU11
D11Mit316
Drg2 Myo15
D11Mit317
B
DRG2
MYO15
100%
75%
50%
0k 2k 4k 6k 8k 10k 12k 14k 16k 18k 20k
MYO15
20k 22k 24k 26k 28k 30k 32k 34k 36k 38k 40k
MYO15
40k 42k 44k 46k 48k 50k 52k 54k 56k 58k 60k
MYO15
60k 62k 64k 66k 68k 70k 72k 74k 76k 78k 80k
MYO15
mouse ESTs
80k 82k 84k 86k 88k 90k 92k 94k 95255

Genomic DNA sequences were analyzed for expressed sequences with the GENSCAN program (Burge and Karlin, 1998) and with BLAST 2.0 (Altschul *et al.*, 1997). After interspersed repetitive elements were masked, GENSCAN accurately predicted 59 of the 65 *MYO15* coding exons that were recovered in cDNA clones. Four additional exons (5, 9, 34, and 45) were predicted by GENSCAN and found in cDNAs but discrepancies existed between actual and predicted donor or acceptor splice sites. Exons 8 and 59 were identified in cDNA clones but were not predicted by the GENSCAN program.

The neural network promoter prediction (NNPP) program (M. G. Reese, www-hgc.lbl.gov/projects/promoter.html) was used to scan the genomic interval between the *DRG2* polyadenylation signal and the start of the *MYO15* ORF. This program identifies TATA box and transcription initiation elements, predicts a transcription start site, and assigns output sequence probability scores ranging from 0 to 1.0. With repetitive elements masked and the probability score cut-off set at 0.95, a single potential promoter element was identified in the human sequence (score = 0.99). This sequence is conserved in the mouse genome, and the mouse sequence was also predicted by the NNPP program as a potential promoter (score = 0.96).

cDNA analysis. Temporal bones of 1- to 3-day-old mouse pups (C57Bl/6J) were dissected in phosphate-buffered saline (PBS), pH 7.4, and homogenized in Trizol reagent, and total RNA was recovered as described (Life Technologies, Gaithersburg, MD). Poly(A) RNA from cochleae of 18- to 22-week human fetuses was a gift from C. Morton. Oligo(dT) or random-primed first-strand cDNA libraries were constructed using an Advantage RT-for-PCR kit (Clontech Laboratories, Palo Alto, CA). Partial myosin XV cDNAs were isolated by PCR from these libraries with an Advantage cDNA PCR kit (Clontech Laboratories). cDNA fragments were either gel-purified and directly sequenced or cloned into the pGEM T-Easy vector (Promega, Madison WI) prior to sequencing. The human and mouse myosin XV cDNA sequences have been deposited with GenBank under Accession Nos. AF144094 and AF144095.

mRNA analysis. Human poly(A) RNA from adult pituitary gland, liver, and brain was purchased from Clontech Laboratories. Total RNA from whole adult mice pituitaries (Pel Freez Biologicals, Rogers, AR) was extracted with Trizol reagent (Life Technologies). Poly(A) RNA was isolated with an Oligotex mRNA Kit (Qiagen Inc., Valencia, CA), and Northern analysis was performed as described (Ausubel, 1991). cDNA probes labeled with [α-^{32}P]dCTP were prepared using a random priming system (Rediprime II, Amersham-Pharmacia Biotech). Prehybridization and hybridization (10^6 cpm/ml) were carried out at 42°C in Ultrahyb solution (Ambion, Inc., Austin, TX). Blots were washed to a final stringency of 65°C in 0.1× SSC and 0.1% SDS and analyzed by autoradiography. After the mouse Northern blot was hybridized with the human *DRG2* cDNA probe, it was washed at 55°C. Between probings, blots were stripped by heating at 95°C in 0.5% SDS (2× 15 min) and then exposed to film to ensure that probe was adequately removed.

A multiple tissue cDNA panel (Catalog No. K1420; Clontech Laboratories) was used to examine the tissue-specific expression of *MYO15* by RT-PCR. As a positive control, first-strand cDNA from adult human pituitary gland was made with a RT-PCR kit (Catalog No. 11146-024; Life Technologies). To normalize the amount of first-strand cDNA used for PCR, a cDNA from a control gene *G3PDH* was first amplified. Amounts of first-strand cDNA that gave approximately equivalent levels of this control product were then used to amplify a 506-bp cDNA product with primers from *MYO15* exons 29 and 32. PCR amplification was performed with the Clontech cDNA polymerase mix (94°C for 60 s followed by 20 or 26 cycles at 94°C for 20 s, 55°C for 30 s, and 68°C for 60 s), and products were visualized by ethidium bromide staining of agarose gels. After 20 cycles, *MYO15* product was seen only in the pituitary lane. After 26 cycles, product was visible from all of the tissues, although substantially more product was seen from the pituitary gland.

MYO15 mRNA expression in human pituitary was examined by *in situ* hybridization as described (Lloyd *et al.*, 1995; Qian *et al.*, 1996). Digoxigenin 11–UTP-labeled riboprobes were prepared from a *MYO15* cDNA fragment cloned into the pGEM-T Easy vector, and antisense or sense probes were transcribed from the T7 promoter (Riboprobe System, Promega, Madison, WI).

In situ hybridization of mouse embryos was performed as described (Ressler *et al.*, 1994; Sassoon *et al.*, 1988). Heads of 18.5-day mouse embryos were fixed in 4% paraformaldehyde/PBS after the skin and brain were removed. The heads were embedded in paraffin and sectioned at a thickness of 10 μm in the transverse orientation. Riboprobes labeled with α-^{35}S-UTP and α-^{35}S-ATP were prepared from cDNA fragments in pGEM-T Easy (Promega) with T7 RNA polymerase using a RNA transcription kit (Stratagene, La Jolla, CA).

Antibody production and immunolocalization. A *Myo15* cDNA fragment encoding residues 2157–2347 was cloned in-frame with GST in pGEX4T-1 (Amersham-Pharmacia Biotech). The same cDNA fragment was also cloned in-frame with the maltose-binding protein (MBP) in pMAL-c2 (New England Biolabs, Beverly, MA). Expression, extraction, and purification of GST-Myo15 (2157/2347) and MBP-Myo15 (2157/2347) fusion proteins from *Escherichia coli* were performed according to the manufacturers' protocols. The purified GST fusion protein was used to immunize a rabbit, and the MBP protein was used to affinity purify the resulting antiserum (TF1). Antibody PB48 was raised in a rabbit against a synthetic peptide corresponding to Myo15 residues 2380–2402 (GDADLEKPTAIAY-RMKGGGQPGG, Princeton Biomolecules, Columbus, OH). Coupling of MBP-Myo15 protein and the synthetic peptide to agarose beads and affinity purification were performed with the buffers and protocol provided with the AminoLink Plus Immobilization Kit (Pierce, Rockford, IL).

Temporal bones from adult mice (B6C3F1/J) were dissected in Leibovitz L-15 medium. Cochlea were removed and fixed for 1 h in 4% paraformaldehyde in PBS. Organs of Corti were dissected, permeabilized for 0.5 h in 0.5% Triton-X 100 in PBS, and incubated overnight in blocking solution (2% BSA, 5% goat serum in PBS). Samples were then incubated for 1 h in blocking solution containing affinity-purified Myo15 antiserum (~0.01 mg/ml), washed with PBS, and incubated for 40 min with a 1:200 dilution of fluorescein-conjugated donkey anti-rabbit antibody (Amersham Pharmacia Biotech). As controls, primary antibody was omitted (not shown) or the Myo15 antiserum was preadsorbed with a 1:1.6 excess of immunogenic peptide (Fig. 7F). Samples were mounted for microscopy with a Prolong Antifade Kit (Molecular Probes, Eugene, OR). Images were obtained with a Zeiss 410 confocal laser scanning microscope (Figs. 7E, 7G, and 7H) or a Zeiss Axiophot microscope equipped with a ×63, 1.4 numerical aperture objective and a Cellscan (Scanalitics, Inc., Fairfax, VA) fluorescence microscopy imaging system (Fig. 7F).

RESULTS

Genomic and cDNA Analysis

To expedite the characterizations of the human and mouse myosin XV genes, we have compiled 95,255 bp of finished sequence from human chromosome 17p11.2 and 88,406 bp of sequence from the homologous region on mouse chromosome 11 (Fig. 1A and Materials and Methods). Potential coding regions within the genomic DNA were identified by aligning the human and mouse sequences to reveal conserved regions, by querying the sequences against the transcribed sequence databases, and through the use of the GENSCAN gene prediction program (Fig. 1B and Materials and Methods). Primers designed from predicted exon sequences were then used to isolate partial cDNA fragments from first-strand cDNA libraries prepared from human fetal cochleae or mouse inner ears (Fig. 2A). Using this approach, 65 myosin XV coding exons and a 5′ noncoding exon were identified in human and mouse cDNA fragments (Figs. 1 and 2A). The 5′ noncoding exon may be

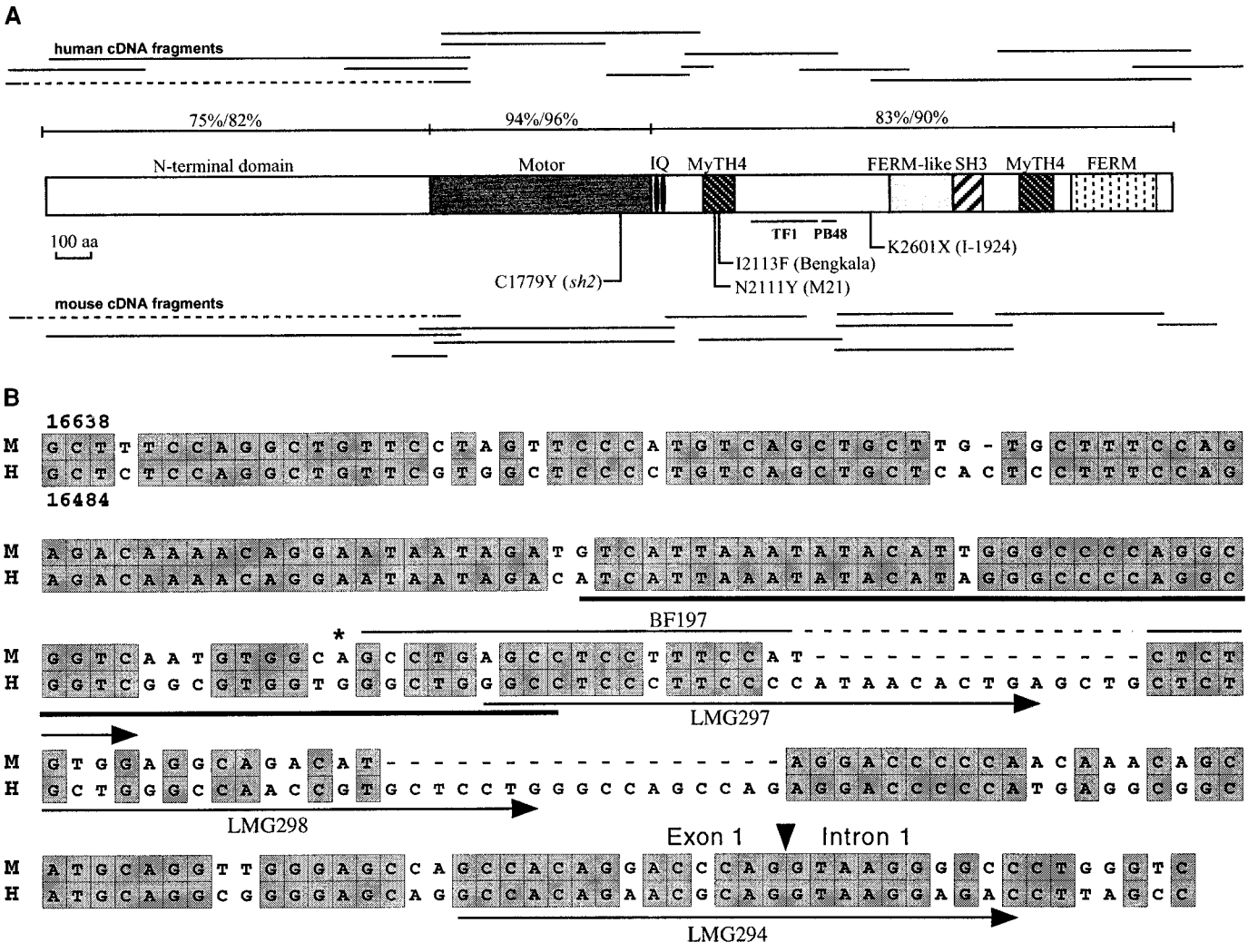

FIG. 2. (**A**) cDNA analysis and myosin XV protein domain structure. The positions of overlapping cDNA fragments isolated by RT-PCR are shown as lines above (human) and below (mouse) a diagram of the myosin XV protein. The hatched lines indicate cDNA fragments spliced directly from exon 1 to exon 3. Amino acid identities/similarities over regions of the human and mouse proteins are indicated above the protein diagram. Amino acid similarities here and in other protein alignments were determined with the ClustalW (BLOSUM matrix) feature of the MacVector program (Oxford Molecular, Campell, CA). The SH3 and FERM domains were identified by querying the human and mouse proteins against the PROSITE database of sequence profiles with ProfileScan (www.isrec.isb-sib.ch/software/PFSCAN_form.html). The region labeled FERM-like is similar to a FERM domain in MYO7A but was not identified as a FERM domain by ProfileScan (see also Fig. 3). The motor, IQ, and MyTH4 domains were recognized via their homology to similar domains in other myosins. The regions of Myo15 used to generate rabbit polyclonal antisera (TF1 and PB48) are indicated. Published human and mouse myosin XV mutations associated with deafness are noted (Probst *et al.*, 1998; Wang *et al.*, 1998). (**B**) Sequence comparison of the human and mouse myosin XV exon 1 genomic regions. A ClustalW alignment of the human (H) and mouse (M) myosin XV exon 1 genomic regions is shown. Identical nucleotides are boxed, and sequences returned as potential promoter elements by the neural network promoter prediction program (NNPP) are underlined. The NNPP predicted transcription start sites are indicated with the asterisk (see also Materials and Methods). The downward pointing arrow shows the position of the exon 1 donor splice site. The sequences of oligonucleotide primers used in RT-PCR to isolate partial human (**bottom**) or mouse (**top**) myosin XV cDNA clones are denoted with arrows. A PCR product was not obtained with primer LMG 294 that spans the exon 1 splice donor site. The genomic nucleotide position of the first base included in the alignment is indicated.

the initial myosin XV exon since it is positioned immediately downstream of a conserved region (86.5% identity over 74 nt) that was identified as a potential promoter element by the neural network promoter prediction program (Fig. 2B and Materials and Methods).

The longest *MYO15* mRNA deduced from overlapping cDNA fragments and the genomic analysis is 11,847 nt, from predicted cap site to polyadenylation signal. This mRNA contains a 10,590-nt open reading frame (ORF, Fig. 2A). The corresponding mouse mRNA is 11,769 nt with a 10,533-nt ORF. An AUG in exon 2, located 339 nt downstream of the predicted transcription start site in the human mRNA, is a good candidate for the myosin XV translation start codon. The sequence context of this AUG is conserved between the human and the mouse genes, and it is identical to the optimal vertebrate translation initiation signal (GCCACC**AUG**G, Kozak, 1996). In both the human and the mouse sequences, in-frame stop codons are found

TABLE 1

Single Nucleotide Polymorphisms (cSNP) and Polymorphic Short Tandem Repeats (STR) in *MTO15*

cSNP	Exon	Variant	Frequency	Forward (F) and reverse (R) primers
D17S2208	17	46051C → T	0.59/0.41	F: CTCCTTCAGATTCAACATGG R: TCTGTGACCTGACTAGGCTC
D17S2209	19	47519C → A	0.59/0.41	F: AGAAGTGAGGAGGATCCAGT R: TGTCTGGCCAAAGCTAAG
D17S2210	41	59772G → A	0.59/0.41	F: TCTCCCTGGATTCTCATTTA R: TCTTTGTCTTCTGTTCCACC
D17S2211	46	63064C → T	0.62/0.38	F: GTATCAGCCACCTCCCTC R: TGAATCCTCTGGACAGGTAG
D17S2212	48	64037C → T	0.62/0.38	F: ATCAGAAGCAGCACAATAGG R: GTCATATTTCCCTGGAACAG
D17S2213	55	67394T → G	0.97/0.33	F: AGAGAATAGAAGCTCCCAGC R: GAACCACAGAGCAGGAAAG
STR	**Alleles**	**Het.**	**Size (bp)**	**Forward (F) and reverse (R) primers**
D17S2207	9	0.89	135–155	F: TATTCTTACCACCTCCCCTG R: CAGGACCTGCTAGTGCAGG
D17S2206	10	0.90	141–165	F: CTGCCTGTCCCTCCACCCACC F: CCTCCCTCCTGGACGCTCTTG

Note. The nucleotide positions are in reference to the 95.2-kb *MYO15* sequence contig (Accession No. AF051976). The six cSNPs are silent changes. Frequencies were determined from 32 chromosomes. For *D17S2207* and *D17S2206,* nucleotide positions 21672 and 38680, respectively, are the first bases of the forward primers. The number of alleles and heterozygosities (Het.) of the STRs were determined from 240 chromosomes.

45 nt upstream of this AUG. The myosin XV ORF ends at a conserved termination codon (UGA) within exon 66. Potential polyadenylation signals (AAUAAA) are present 910 and 948 bp downstream of this position in the human and mouse sequences, respectively (Fig. 1A).

In the course of our sequence analysis, two highly polymorphic dinucleotide repeats and 6 single nucleotide polymorphisms (cSNPs) were identified within the *MYO15* gene. The characteristics of these genetic markers and their nucleotide positions according to the 95.2-kb genomic sequence contig are summarized in Table 1.

An alignment of the human and mouse genomic sequences is presented as a percent identity plot (PIP) in Fig. 1B. This plot graphically illustrates the homology between the coding regions of the human and mouse myosin XV genes, as well as those of *DRG2,* a GTP-binding protein gene adjacent to myosin XV in both genomes. A highly conserved genomic region that has not been recovered in human or mouse cDNA fragments is evident on this plot in the intron between myosin XV exons 2 and 3 (Fig. 1B). A portion of this region contains a conserved ORF flanked by potential 5′ and 3′ splice sites and may be included as an exon in some myosin XV transcripts.

Myosin XV Protein Structure

The protein encoded by the deduced *MYO15* mRNA is composed of 3530 amino acids and has a calculated molecular mass of 395.1 kDa. The corresponding mouse protein is composed of 3511 amino acids and shares 82% overall identity with the human protein (Fig. 2A). The most striking feature of the myosin XV proteins, in relation to other myosins, is the presence of a very long N-terminal extension preceding the conserved motor domain. The predicted N-terminal regions of the human and mouse proteins are 76% identical and are composed of 1223 and 1208 amino acids, respectively. In both species, the N-terminal extensions have a high proline content (~17%) and are encoded primarily by the GC-rich exon 2 (see Fig. 1B). Except for weak matches to proline-rich regions in other proteins, they show little similarity to sequences in the protein databases.

The motor domains of the human and mouse myosin XV proteins are 94% identical (Fig. 2A) and are most closely related to the motor domain of bovine myosin X (41.2% identity for MYO15). Like other myosins, the myosin XV motor domain contains regions predicted to function as ATP- and actin-binding sites (Cope *et al.,* 1996; Probst *et al.,* 1998; Wang *et al.,* 1998). Immediately following the motor domain are two regions (1909-**LQ**RCL**RG**FFI**KR** and 1932-**LQ**SRA**RG**YLA**RQ** in MYO15) that closely resemble the myosin light chain-binding site consensus sequence (IQxxxRGxxxRK, Mooseker and Cheney, 1995). Precedent from other myosins suggests that these sequences mediate binding to calmodulin or other members of the EF-hand family of calcium-binding proteins (Houdusse *et al.,* 1996).

The tail domains of the human and mouse myosin XV proteins are composed of 1587 and 1584 amino acids, respectively. Over the lengths of their tails, the human and mouse proteins are 83% identical (Fig. 2A). BLAST searches and protein alignments revealed that

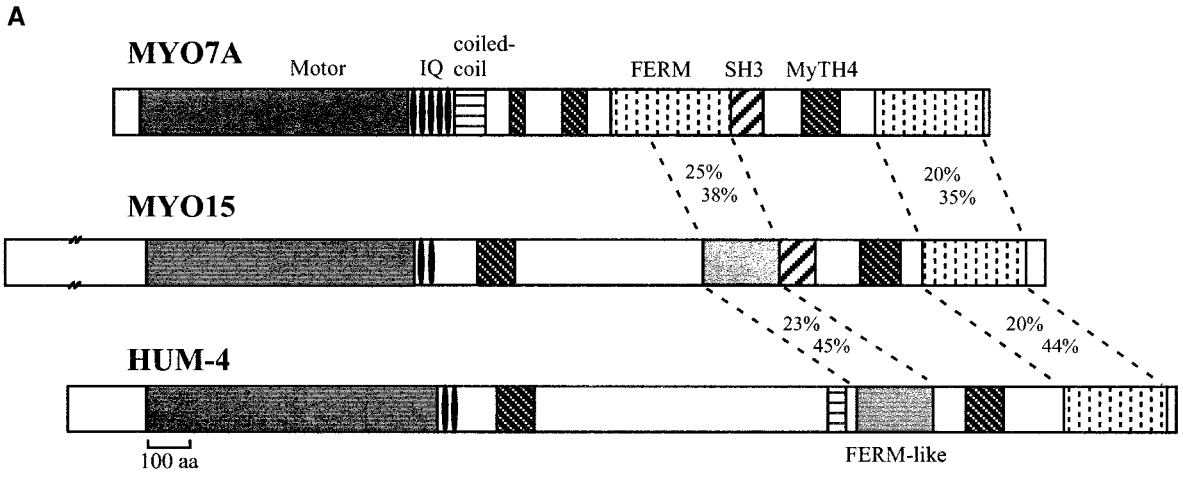

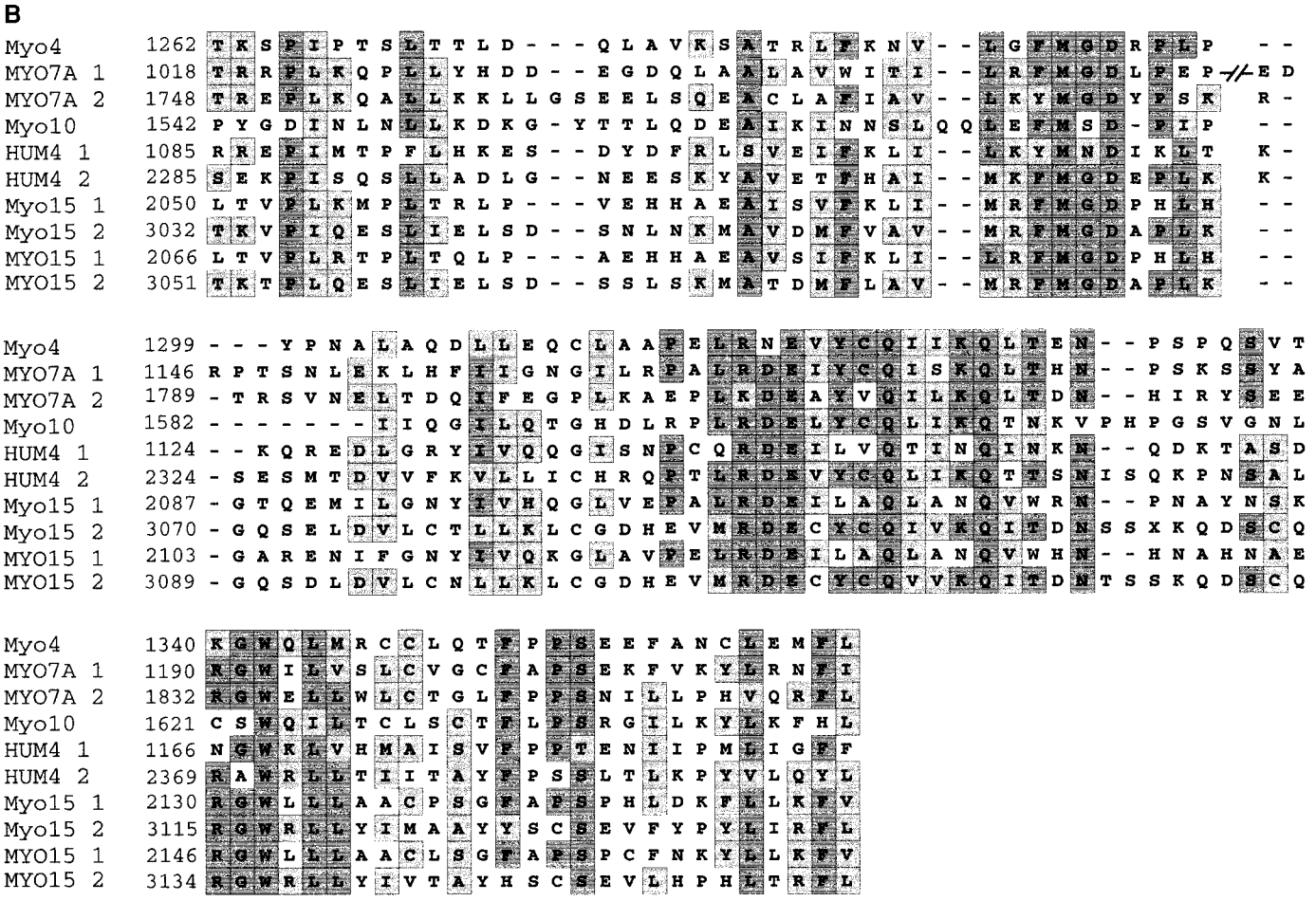

FIG. 3. (**A**) Comparison of the domain structures of MYO15, MYO7A, and HUM-4. Percentage amino acid identities (**top**) and similarities (**bottom**) of regions in MYO7A and HUM-4 relative to MYO15 are indicated. The FERM domain in HUM-4 was identified with ProfileScan (see Fig. 2A). Other domains in HUM-4 and MYO7A have been previously described (Baker and Titus, 1997; Chen *et al.*, 1996; Mburu *et al.*, 1997). No regions with a propensity to form coiled-coil α-helices were detected with the PairCoil program (Berger *et al.*, 1995) in the myosin XV tail, indicating that myosin XV may function as a single-headed myosin. (**B**) ClustalW alignment of the MyTH4 domains in unconventional myosins. Identical amino acids are dark shaded, and similar residues are light shaded. The first MyTH4 domain in MYO7A has an 88-amino-acid insertion (Chen *et al.*, 1996) that is not included in the alignment. *Acanthameoba* myosin-4 (M60954); *Hs* MYO7a (U39226); *B. taurus* myosin-X, (U55042); *C. elegans* HUM4 (myosin-XII, Z66563). (**C**) ClustalW alignment of the putative myosin XV SH3 domain with SH3 domains in other proteins. The alignment reveals several residues in myosin XV that are highly conserved in SH3 domains. The myosin XV domain also contains an insertion at the same position as an insertion in the PI3K SH3 domain (Liang *et al.*, 1996). *Rn* PI3K, phosphatidylinositol 3-kinase (Q63787); *Hs* ArgBP2a, Arg/Abl-interacting protein (AF049884); *Gg* Cortactin, Src substrate p80/85 protein (M73705); *Hs* GRB2, epidermal growth factor receptor-binding protein (M96995); *Hs* SH3P17, an SH3 domain-containing protein (U61166); *Sc* Myo5p, a type I myosin (NCBI protein database Accession No. 1699241); *Ac* HMW IV, high-molecular-weight myosin-4 (J05678); *Hs* MYO7A (U39226). GenBank accession numbers are provided in parentheses after each protein.

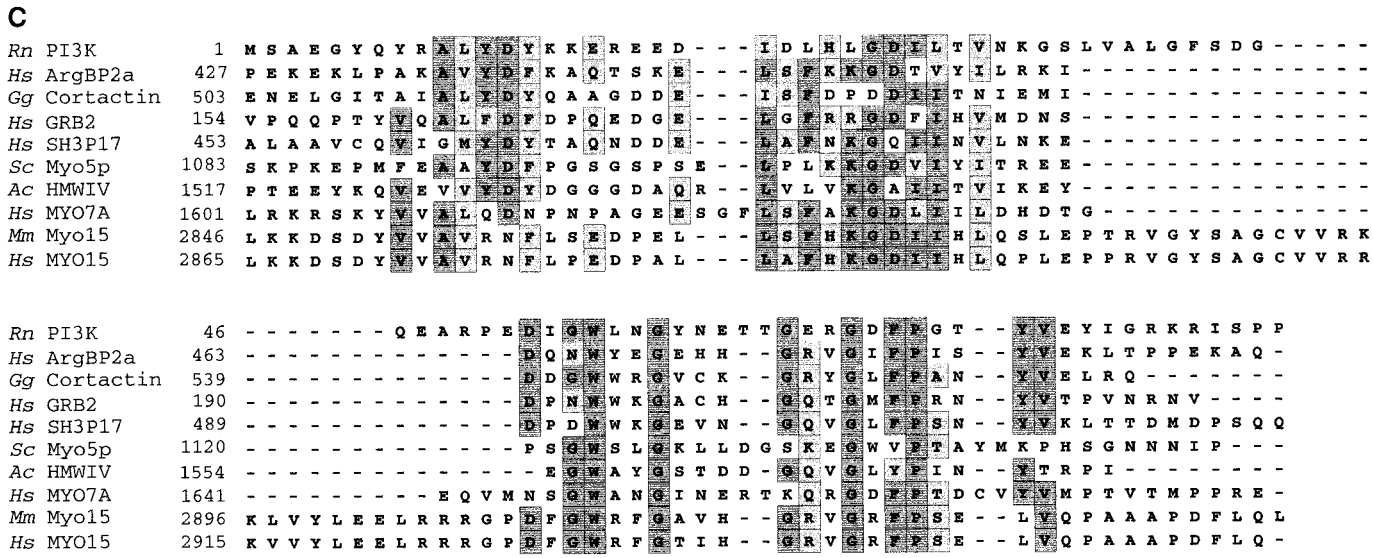

FIG. 3—*Continued*

the myosin XV tail regions were similar to the tails of *Caenorhabditis elegans* myosin XII (HUM-4) and myosin VIIA (MYO7A). This similarity is most evident in two myosin tail homology 4 (MyTH4) domains and in two regions that, in MYO7A, have been termed talin-like domains (Chen *et al.*, 1996). MyTH4 domains are present in the tails of several unconventional myosins, but their function(s) remains unknown (Chen *et al.*, 1996). The talin-like domains, on the other hand, are similar to a membrane attachment FERM domain conserved in talin, protein 4.1 (band 4.1), and members of the ezrin, radixin, and meosin family of cytoskeleton-associated proteins (Chen *et al.*, 1996; Chishti *et al.*, 1998; Mburu *et al.*, 1997). Similarities among the tails of MYO15, MYO7A, and HUM-4, including regions with homology to the FERM domain, are illustrated in Fig. 3A. A comparison of the myosin XV MyTH4 domains to those of other unconventional myosins is given in Fig. 3B.

A potential protein interaction motif in the form of an SH3 domain was also identified in the tail regions of the human and mouse myosin XV proteins immediately following the first FERM-like domain (Fig. 3A). A putative SH3 domain has also been identified at a similar position in myosin VIIa (Mburu *et al.*, 1997). An alignment of these regions to a selection of SH3 domains from other proteins is shown in Fig. 3C. This alignment reveals several residues in the myosin XV SH3 regions that are highly conserved among SH3 domains (Musacchio *et al.*, 1992). The protein and mRNA positions of all of the potential domains identified in MYO15 are given in Table 2.

Alternative Processing of Myosin XV Transcripts

In our analysis of inner ear *MYO15* cDNAs, several alternatively spliced transcripts were identified. As examples, cDNAs individually missing exons 2, 8, 26, 30, 40, and 61 were recovered. In the case of exons 30, 40, or 61, the exon skipping produces a reading frameshift, terminating the *MYO15* ORF shortly downstream of the missing exon. Skipping of exons 2, 8, or 26, on the other hand, does not interrupt the *MYO15* reading frame. While it is difficult to assess the significance of these alternatively spliced transcripts, some appear worthy of further consideration. Both cDNA and Northern blot analyses, for example, support the alternative inclusion of exon 2 in mRNAs. Exon 2 contains the myosin XV translation start codon and encodes most of the myosin XV N-terminal domain. In transcripts without exon 2, the first AUG in-frame with the myosin XV ORF is located at the beginning of exon 3 (Fig. 4A). The context of this AUG is similar in the mouse and human transcripts (human sequence, ACCCAG/**AUG**CAC; mouse sequence, ACGCAG/**AUG**CAG, where the slash indicates the exon 1/exon 3 junction). Starting translation at this position would produce a protein with 20 residues preceding the conserved motor domain.

Alternative splicing of exons 8 and 26 has also been

TABLE 2

Exon Locations of MYO15 Domains

Domain	Exon	Nucleotide	Amino acid
N-terminal domain	2–3	337–4007	1–1223
Motor	3–24	4,008–6,035	1224–1899
ATP-binding site	7	4,281–4,304	1315–1322
Actin-binding site	17	5,304–5,327	1656–1663
IQ motif 1	24	6,063–6,095	1909–1919
IQ motif 2	24	6,132–6,164	1932–1942
MyTH4 domain 1	29–31	6,534–6,860	2066–2174
FERM-like	43–48	8,397–8,939	2687–2867
MyTH4 domain 2	53–57	9,489–9,821	3051–3161
SH3 domain	49–51	8,931–9,215	2865–2959
FERM	59–65	9,987–10,829	3217–3497

Note. Nucleotide positions are according to the *MYO15* cDNA (GenBank Accession No. AF144094).

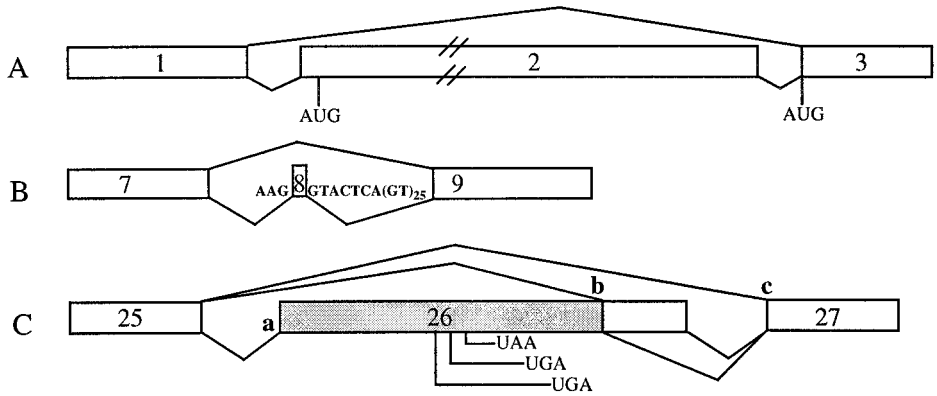

FIG. 4. Schematic representation of alternative splicing events identified in human and mouse myosin XV cDNAs. (**A**) Alternative splicing resulting in the inclusion or exclusion of the ~3800-nt exon 2 in myosin XV. The positions of predicted translation start codons in exons 2 and 3 are indicated. (**B**) Alternative splicing of the 6-nt exon 8 (ATAAAG). The intronic sequences flanking human exon 8 are depicted. The GT dinucleotide repeat following the splice donor site is *D17S2206* (see Table 2). Seven GT dinucleotide repeats are also found at this position in the mouse sequence [AAG/ATAAAG/GTATGCTG$(GT)_7$]. (**C**) Alternative splicing involving exon 26. Three alternative splice acceptor sites (a, b, and c) are used with the donor splice site following exon 25.

observed in both human and mouse cDNAs. Exon 8 is 6 nt, and its inclusion introduces a 2-amino-acid insertion in the myosin XV motor domain. When positioned on the framework of the chicken fast skeletal myosin II crystal structure, this insertion falls within an unresolved variable surface loop (residues 200–220) at the junction of the 25- and 50-kDa proteolytic cleavage products (Cope *et al.*, 1996; Rayment *et al.*, 1993). Vertebrate nonmuscle myosin IIB and smooth muscle myosin II isoforms also have insertions within this loop as a result of alternative splicing (reviewed in Sellers, 1999). A 7-amino-acid insertion at this position in avian smooth muscle myosin II has been shown to impact markedly the *in vitro* motility properties of the protein (Kelley *et al.*, 1993).

In the case of exon 26, alternative splice acceptor usage results in a long form of the exon (216 nt in humans and 189 nt in mice), a short form of the exon (54 nt), or exon skipping (Fig. 4C). Inclusion of the short form of exon 26 introduces an 18-amino-acid insertion C-terminal to the second IQ motif compared to transcripts without exon 26. A translation termination codon is introduced into the myosin XV ORF in the long form of exon 26 (Fig. 4C). Translation of transcripts containing this version of the exon would produce a protein that is truncated shortly after the IQ motifs.

Read-through Transcription into MYO15

In both the human and the mouse genomes, a gene, *DRG2*, encoding a putative GTP-binding protein is found immediately upstream of myosin XV (see Fig. 1). The *DRG2* polyadenylation signal is located just 755 and 1137 bp upstream of myosin XV exon 1 in the human and mouse sequences, respectively. In our attempts to identify the 5′ end of the human *MYO15* mRNA using rapid amplification of cDNA ends (RACE), two classes of products were obtained. In one class, sequences from the 3′ portion of *MYO15* exon 2 were found spliced to exon 3 and downstream exons. These products likely arise from incomplete first-strand cDNA synthesis. The second class of RACE products were hybrid cDNA fragments containing *DRG2* exons fused to *MYO15* exons. In all of these products, another exon (nt 23907–23974) derived from a repetitive LINE element in *MYO15* intron 1 was present between the *DRG2* and the *MYO15* sequences. This intermediate exon contained translation termination codons in all three reading frames, indicating that these transcripts do not likely encode DRG2/MYO15 fusion proteins. We hypothesize that these transcripts result from transcription read-through from the *DRG2* gene into the *MYO15* gene and that they are not functionally significant. Their existence, however, has complicated the identification of the 5′ end of the *MYO15* gene.

Analysis of Myosin XV mRNA Expression

To determine the tissue distribution of *MYO15* mRNA expression, a dot blot with poly(A) RNA from 50 adult and fetal tissues was sequentially hybridized with radiolabeled cDNA probes from the N-terminal (exon 2) or tail (exons 31–41) regions of *MYO15*. With both probes, hybridization signals were detected primarily in mRNA from adult pituitary gland (Fig. 5A), although with longer exposure times some signal was also detected in RNA from testis and ovary (not shown). The blot was next hybridized with a cDNA probe from the *DRG2* gene. This probe was chosen because we had earlier identified 5′ RACE products containing *DRG2* exons fused out of frame to *MYO15* exons. While we believe that these RACE products were derived from nonfunctional read-through transcripts, it was also possible that they were responsible for the *MYO15* hybridizing signal observed on the dot blot. The *DRG2* probe, however, hybridized to mRNA from all of the adult and fetal tissues on the blot,

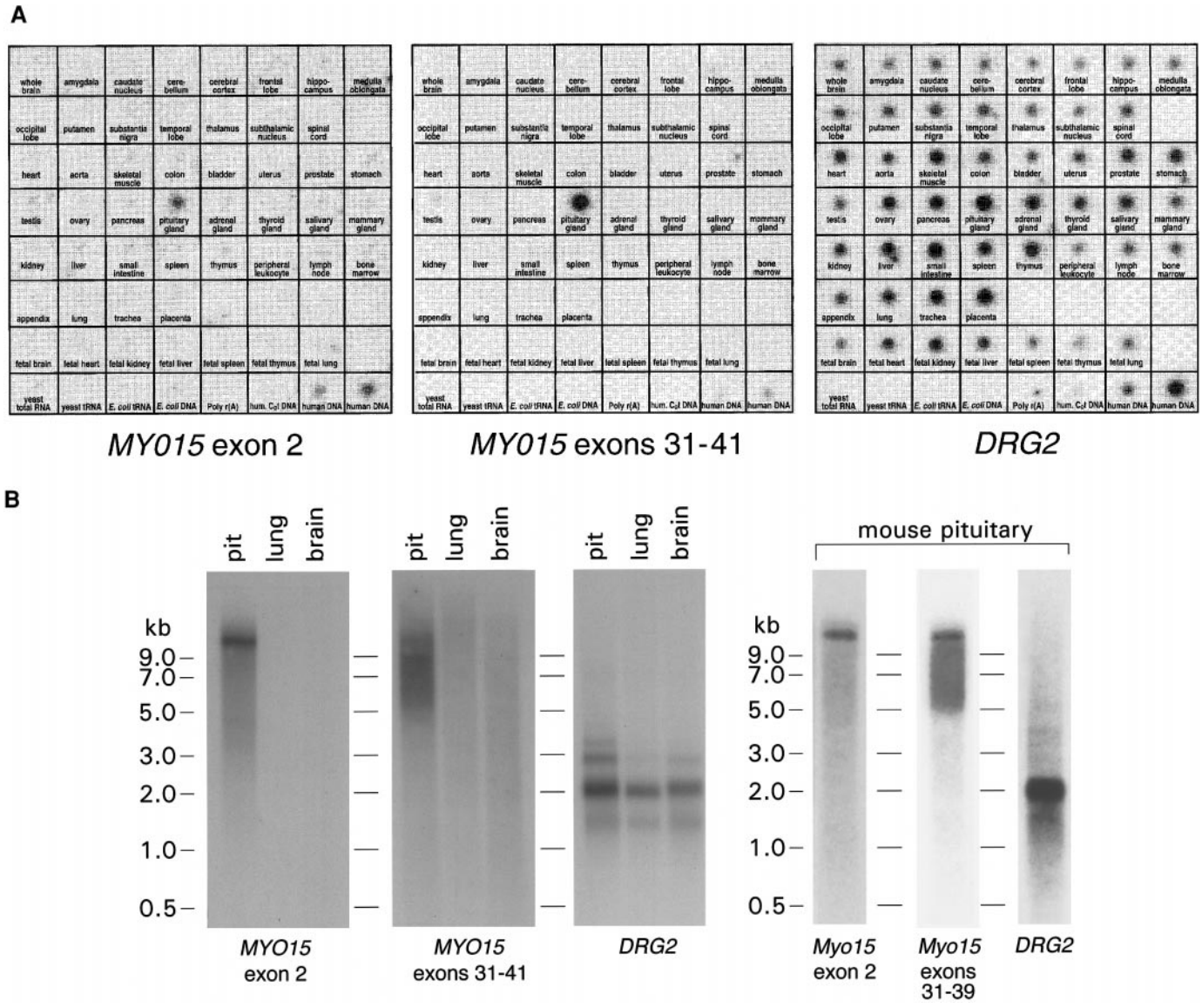

FIG. 5. Tissue distribution and Northern blot analysis of myosin XV mRNA. (**A**) A multitissue dot blot (Clontech) was sequentially hybridized with the indicated radiolabeled cDNA probes. The *MYO15* probes were derived from regions of the *MYO15* cDNA (GenBank Accession No. AF144094) encoding portions of the N-terminal (exon 2, nt 408–1772) or the tail domains (exon 31–41, nt 6992–8198). The *DRG2* probe included nt 19–1311 of a published cDNA (Schenker *et al.*, 1994). (**B**) Northern blots were prepared with poly(A) RNA (~2.5 μg/lane) from the indicated human or mouse tissues. The Northern blot with mRNA from human tissues was sequentially hybridized with the same probes used in the dot blot analysis. The mouse blot was hybridized with probes from the N-terminal (exon 2, nt 288–1072) and tail regions (exons 31–39, nt 6758–7739) of the predicted full-length *Myo15* cDNA (GenBank Accession No. AF144095). As a control, this blot was also hybridized with the human *DRG2* cDNA probe. RNA molecular weight standards are indicated.

indicating that the *MYO15* hybridization signal observed from pituitary gland mRNA did not likely result from *DRG2*/*MYO15* read-through transcripts.

The tissue distribution of *MYO15* expression was also examined by RT-PCR. Under amplification conditions where *MYO15* cDNA product was readily detected from human pituitary gland, no products were observed from adult human brain, kidney, liver, lung, pancreas, placenta, or skeletal muscle (data not shown; see Materials and Methods). However, with additional amplification cycles, low levels of *MYO15* products relative to the amount detected from the pituitary gland were observed from each of these tissues (data not shown). The biological significance of the low level of *MYO15* expression in these tissues is not known.

The dot blot and RT-PCR analyses indicated that adult human pituitary gland might be a useful source of *MYO15* mRNA for Northern analysis since mRNA from human inner ear is difficult to obtain and *Myo15* expression is limited to just a few cells in the inner ear (see below). A Northern blot was therefore prepared with mRNA from adult pituitary, lung, and brain and sequentially hybridized with the same probes used in the dot blot analysis (Fig. 5B). The *MYO15* exon 2

probe hybridized to an approximately 12-kb RNA species from pituitary gland. The size of this transcript is consistent with the predicted size of the full-length *MYO15* mRNA [~11.9 kb not including a poly(A) tail]. A similar signal was also detected when the blot was hybridized with the probe from the *MYO15* tail region. In addition, the tail probe hybridized to a broad region ranging from approximately 5 to 9 kb. These results suggest that both the upper (~12 kb) and the lower (~5–9 kb) hybridization signals contain sequences from *MYO15* exons 31–41, but that only the upper signal contains exon 2 sequences. This interpretation is consistent with the alternative inclusion of the 3828-nt exon 2 that we observed in our cDNA analysis. Possible explanations for the broad size range of the lower hybridization signal (5–9 kb) include alternative processing of myosin XV transcripts, resulting in a range of transcript sizes, and/or partial degradation of transcripts that do not include exon 2.

The *DRG2* control probe hybridized with a major transcript of ~2.0 kb that was present in all of the tissues represented on the Northern blot (Fig. 5B). Similar results were obtained with four independently prepared Northern blots with mRNA from human pituitary gland and with a Northern blot containing poly(A) RNA from adult mouse pituitary gland (Fig. 5B).

Distinct *MYO15* hybridization signals were not detected by dot blot or Northern analysis in mRNA from adult brains (Fig. 5B). This result was unexpected because we had previously observed *MYO15* hybridization signals of 4.5–5.5 kb on Northern blots with mRNA from human brain (Wang *et al.*, 1998). We believe that the most likely explanation for this discrepancy is that the probe used in the previous Northern analyses cross-hybridized to a non-*MYO15* transcript. The probe used in the earlier experiments was derived from *MYO15* exons 31–51 and included cDNA sequences encoding regions of the MYO15 FERM-like and SH3 domains (see Table 2). In contrast, the probes used in the current set of experiments were chosen from regions of the *MYO15* transcript that do not encode recognizable protein domains.

MYO15 expression in normal adult human pituitary gland was further examined by *in situ* hybridization with an antisense riboprobe from *MYO15* exons 31–41. As shown in Fig. 6A, *MYO15* mRNA was detected in the cytoplasm of many anterior pituitary gland cells. In contrast, very little hybridization signal was observed with this probe in liver cells or in the pituitary gland with the corresponding sense probe (Figs. 6B and 6C). The conserved expression of myosin XV in the pituitary gland indicates a function for myosin XV in this tissue. Although an abnormal pituitary phenotype has not been noted in humans or mice homozygous for myosin XV mutations, a clinical examination of pituitary function may now be warranted in *DFNB3* individuals presumed to have nonsyndromic deafness.

Myosin XV Expression in the Mouse Inner Ear

To examine *Myo15* transcript expression in the developing inner ear, antisense *Myo15* riboprobes from exon 2 or exons 48–51 were hybridized *in situ* to paraffin-embedded sections of heads from 18.5-day postcoitum (dpc) mouse embryos (Figs. 7A–7D). With both probes, positive hybridization signals were detected in restricted regions of the developing cochleae and vestibular apparatus. Although identifying specific cell types was difficult on the slides processed for *in situ* hybridization, the signal appeared to be limited to the region of the cochlear neurosensory hair cells and to the upper epithelial layer of the macula sacculi (Figs. 7A and 7C). On other sectional planes, hybridization signals were also detected within the macula utriculi and cristae ampullaris of the three semicircular canals (data not shown). Similar inner ear hybridization signals with both probes were detected on sections prepared from of 15.5-dpc and day 1 postnatal mice (data not shown). In all of the experiments, the hybridization signals observed with the exon 2 probe were less intense than those seen with the tail-derived probe (e.g., compare Figs. 7A and 7C). This difference may indicate that transcripts containing exon 2 represent a subset of *Myo15* transcripts in the inner ear. Alternatively, the different intensities might be explained by differences in the specific activities or hybridization properties of the probes.

Expression of Myo15 protein in whole-mount cochlear tissue from adult mice was examined by indirect immunofluorescence with affinity-purified, polyclonal antibodies directed against two regions of the Myo15 tail (see Fig. 2A and Materials and Methods). Both antibodies (TF1 and PB48) labeled the same structures within cochlear inner and outer hair cells (Figs. 7E–7H). Labeling was most intense in the microvillus-like extensions of the hair cells, the stereocilia (Figs. 7E and 7F), and within the apical cell body in the region of the cuticular plate (Fig. 7G). Diffuse staining was also observed throughout the cytoplasm of the hair cells. In contrast, little fluorescence was observed in supporting cells or other cell types in the organ of Corti. With antibody PB48, but not with TF1, an unidentified punctate structure at the base of the outer hair cells was also labeled (not shown). The localization of Myo15 in cochlear sensory hair cells is consistent with the deafness phenotype of *sh2* mice and the expression pattern of *Myo15* transcripts observed by *in situ* hybridization.

DISCUSSION

The human and mouse myosin XV genes contain 66 exons and span 71 and 60 kb of genomic DNA, respectively. Composite full-length myosin XV cDNAs are approximately 12 kb and encode proteins with calculated molecular masses of about 400 kDa. Like other members of the myosin superfamily, the human and

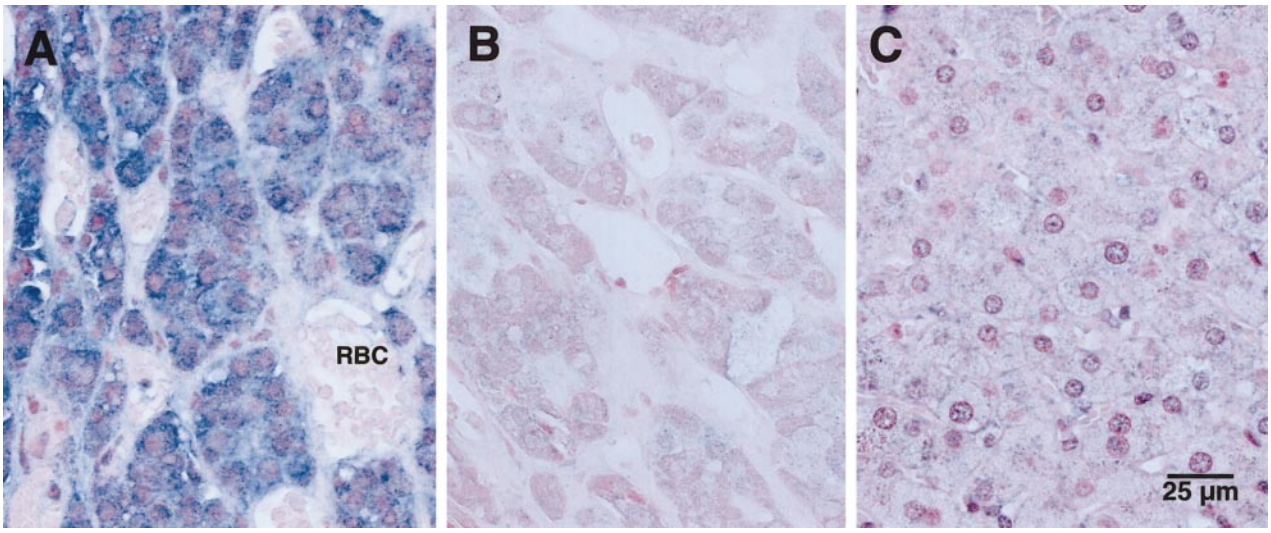

FIG. 6. Expression of *MYO15* mRNA in anterior pituitary cells. (**A**) *In situ* hybridization with a digoxigenin-labeled antisense riboprobe (*MYO15* exons 31–41, nt 6992–8198) revealed diffuse cytoplasmic staining (blue) of varying intensities in different anterior pituitary gland cells. Red blood cells (RBC) in capillaries were negative for *MYO15* expresssion. (**B**) Hybridization with the corresponding sense probe was negative for staining. (**C**) Hybridization of liver cells with the antisense *MYO15* probe was also largely negative for staining. In all panels, nuclei were counterstained with nuclear fast red, and the *in situ* hybridization signal was detected with nitroblue tetrazolium and 5-bromo-4-chloro-3-indolyl phosphate (NBT/BCIP).

mouse myosin XV proteins contain conserved motor domains, light chain-binding sites (IQ motifs), and C-terminal tail domains. A novel feature of myosin XV, however, is the presence of more than 1200 amino acids preceding the conserved myosin motor domain. With the exception of class III myosins such as *Drosophila melanogaster* ninaC, the motor domains of known myosins are located within 200 amino acids of the N-terminus, and specific functions for sequences prior to the motor domains have not been described (Mermall *et al.*, 1998; Mooseker and Cheney, 1995). The 333-amino-acid ninaC N-terminal domain possesses a kinase activity that is mutationally separable from the activity of the motor domain and is required for normal phototransduction in *Drosophila* eye cells (Montell and Rubin, 1988; Porter and Montell, 1993). The size and evolutionary conservation of the myosin XV N-terminal region suggest that it also has a distinct function. The primary amino acid sequence of this region, however, provides few clues as to what this function might be. Furthermore, as indicated by our expression and cDNA analyses, myosin XV isoforms with and without the N-terminal extension may exist in the same cells. Clearly, further experimentation is needed to determine the proportion of proteins containing the N-terminal extension and the role this region plays in myosin XV function.

The myosin XV tail contains a combination of MyTH4 and FERM-like domains that are also present in myosin XIIA and *C. elegans* myosin XII (HUM-4; Baker and Titus, 1997; Chen *et al.*, 1996; Mburu *et al.*, 1997; Weil *et al.*, 1995). A similar set of domains has been noted in the tail domains of bovine myosin-X and several plant kinesin-like proteins (Chen *et al.*, 1996; Mburu *et al.*, 1997). The coexistence of MyTH4 and FERM-like domains in this diverse group of motor proteins suggests that these domains may be functionally linked and that the tails of these proteins may interact with similar cellular components.

To date, MyTH4 domains have been found only in myosin and kinesin-like motor proteins, and a function for the domain has not been determined. In contrast, the FERM domain was originally identified in a group of proteins (band 4.1, talin, merlin and the ezrin, radaxin, meosin family of proteins) believed to function as linkers between the cytoskeleton and the plasma membranes (reviewed in Chishti *et al.*, 1998). In these proteins, one role of the FERM domain is to mediate

FIG. 7. *Myo15* expression in the mouse inner ear. (**A–D**) *In situ* hybridization of paraffin embedded ~18.5-day mouse embryo heads with radiolabeled riboprobes transcribed from cDNA fragments encoding portions of the *Myo15* N-terminal (exon 2; nt 288–1072) or tail (exons 48–51, nt 8726–9199) domains. Dark-field images are shown with Hoechst staining used to reveal nuclei. The sections shown are consecutive 10-μm sections from the same mouse. (**A**) N-terminal domain antisense probe. (**B**) N-terminal domain sense probe. (**C**) Tail domain antisense probe. (**D**) Tail domain sense probe. With both antisense probes, but not with the corresponding sense probes, hybridization signals were observed in the same cells within limited regions of the cochleae (arrowheads) and in the vestibular apparatus in the region of the macula sacculi (arrows). (**E–H**) Localization of Myo15 in cochlear hair cells by indirect immunofluorescence of whole-mount preparations of adult mouse organ of Corti. (**E**) Immunolabeling within the stereocilia of the single row of inner hair cells (IHC) and three rows of outer hair cells (OHC) with anti-Myo15 antibody TF1. (**F**) High-magnification view of outer hair cell stereocilia labeled with anti-Myo15 antibody PB48. (**G**) Labeling within the apical cell body in the actin-rich region of the cuticular plate in both inner and outer hair cells with antibody TF1. A very similar labeling was detected at this focal plane with the PB48 antibody (not shown). (**H**) Blocking of TF1 labeling by preincubation with immunogenic peptide. The focal plane of this image is the same as that shown in **G.**

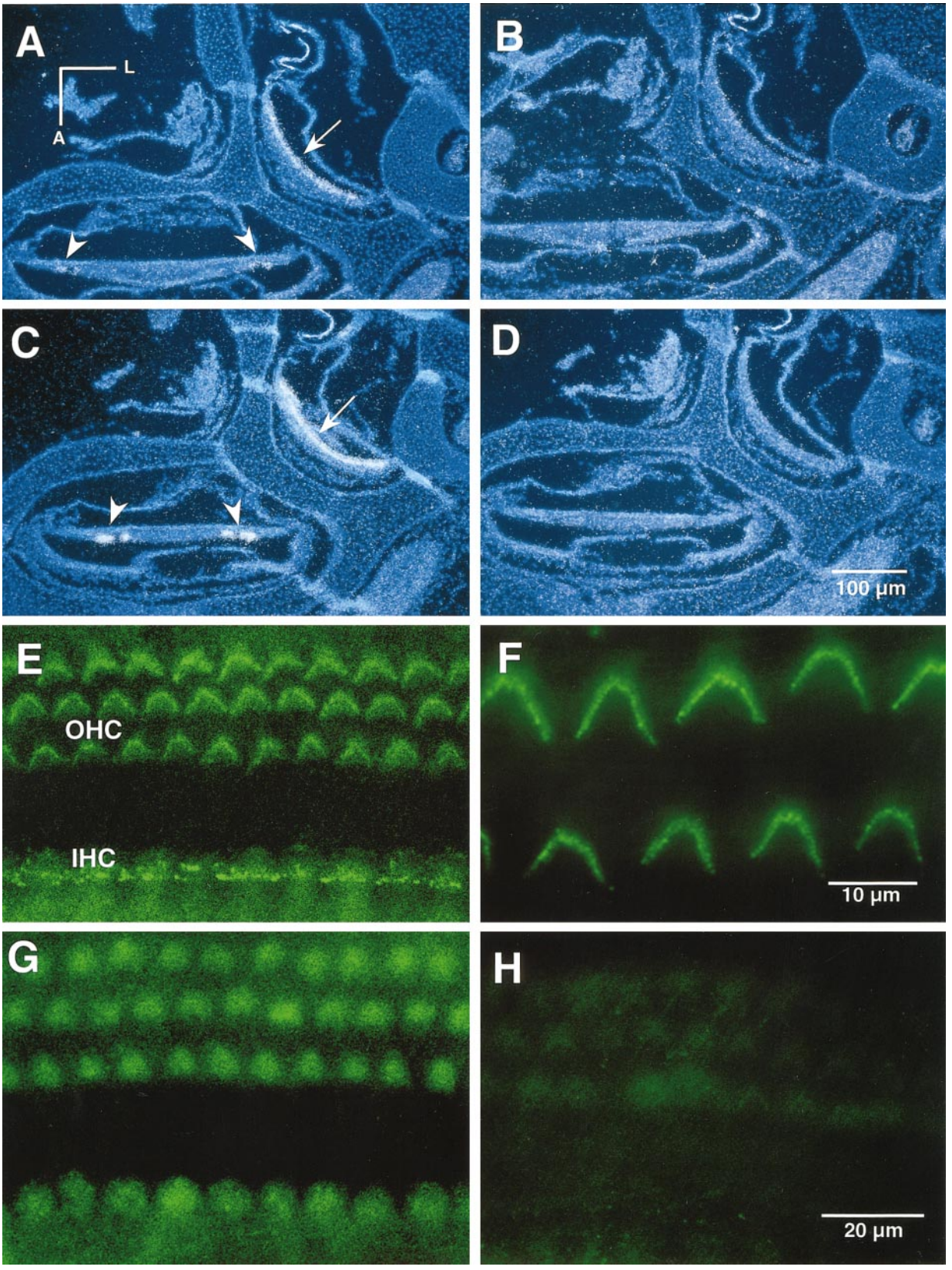
A
L
A
B
C
D
100 μm
E
OHC
IHC
F
10 μm
G
H
20 μm

membrane attachment via specific binding to integral membrane proteins. A related function for the FERM-like domains of unconventional myosins would be consistent with membrane trafficking roles predicted for at least some of these proteins (Mermall *et al.*, 1998).

A putative SH3 domain is also present in the myosin XV tail. SH3 domains mediate the assembly of protein complexes by binding proline-rich peptide sequences and have been found in numerous proteins with wide-ranging functions (reviewed in Dalgarno *et al.*, 1997; Mayer and Gupta, 1998). In addition to myosin XV, class IV, class VII, and some class I myosins contain SH3 domains (Mermall *et al.*, 1998). The SH3 domain in the yeast class I myosin, Myo5p, plays a role in protein localization and mediates binding to a proline-rich, actin-binding protein, verprolin (Anderson *et al.*, 1998). A protein partner of unknown function, Acan125, has also been described for the *Acanthamoeba* myosin-1C SH3 domain (Xu *et al.*, 1997). While the function of the myosin XV SH3 domain is unknown, an intriguing possibility is that it mediates an intramolecular interaction with a region of the proline-rich N-terminal domain. A similar self-association between a proline-rich region and a SH3 domain in the signaling protein phosphoinositide 3-kinase (PI3K) has been proposed to play a role in regulating PI3K activity (Kapeller *et al.*, 1994). Precedent also exists for myosin activity to be regulated by intramolecular folding. Under some conditions, the long tails of smooth muscle and nonmuscle myosin II molecules can fold back upon the neck region of the head, forming a more compact molecule with suppressed enzymatic activities (Olney *et al.*, 1996; Trybus *et al.*, 1982). Similarly, kinesin, a microtubule-dependent motor, has folded and extended states (Hackney *et al.*, 1992).

By *in situ* hybridization, we observed *Myo15* expression in the neurosensory epithelial regions of the cochlea, saccule, utricle, and cristea ampularis of the developing mouse inner ear. This expression pattern is consistent with the auditory and vestibular phenotypes of *sh2* mice and also with the Myo15 immunolocalization reported here. With two independent Myo15 antibodies, immunolabeling was observed within the stereocilia and cuticular plate regions of adult cochlear inner and outer hair cells, the primary sensory cells of the auditory system. Hair cell stereocilia are microvillus-like cellular processes that form a highly organized bundle extending from the apical surface of the cell. Mechanical deflection of the stereociliary bundle in response to sound is believed to open or close ion channels on the stereocilia, thus inducing an electrical impulse that is transmitted to the central nervous system (reviewed in Hudspeth, 1992; Hudspeth and Gillespie, 1994). The cores of stereocilia consist of numerous cross-linked actin filaments that appear to be anchored within the hair cell body in another actin-rich region, the cuticular plate (DeRosier and Tilney, 1989; Hasson *et al.*, 1997). In *sh2* mice, the stereociliary bundles of cochlear hair cells are present and well ordered, but the individual stereocilia are much shorter than those of wildtype hair cells (Probst *et al.*, 1998). In addition, an abnormal intracellular actin rod-like structure extending toward the base of the cell is present in *sh2* inner hair cells (Probst *et al.*, 1998). These structural anomalies, together with the localization of Myo15 within the hair cell stereocilia, suggest a role for Myo15 in the proper organization or assembly of the actin filaments that comprise the core of the stereocilia. A potential role for Myo15 in the formation or maintenance of the lattice of actin filaments that comprise the cuticular plate is also suggested by its presence in this region of the cell.

Preliminary data indicate that, in a sample of 82 Indian and Pakistani families segregating recessive deafness, up to 10% may be linked to *DFNB3* (E. R. Wilcox, pers. comm., Rockville, 1999). Thus, mutations in *MYO15* may be responsible for a relatively large proportion of hereditary deafness. The elucidation of the genomic and cDNA structures reported here is essential for the identification of additional *MYO15* mutations and an accurate assessment of the extent to which *DFNB3* contributes to hereditary deafness worldwide.

ACKNOWLEDGMENTS

We thank J. R. Lupski and K.-S. Chen for the human chromosome 17 cosmid library. We are grateful to J. Kim for help in dissecting mouse temporal bones and to D. K. Wu for discussions and help in interpreting *in situ* hybridization data. We thank E. Wilcox for sharing unpublished data and are grateful to D. Drayna, J. Battey, R. Wenthold, A. Griffith, R. Morell, and members of the LMG for insightful comments. This work was supported by National Cancer Institute Grants CA 42951 and CA37231 (R.V.L.), National Institute of Child Health and Human Development Grant R01 HD30428 (S.A.C.), and the National Institute on Deafness and Other Communication Disorders Intramural Research Projects Z01 DC 00035-02, Z01 DC 00039-02, and Z01 DC 00048-01.

REFERENCES

Altschul, S. F., Madden, T. L., Schaffer, A. A., Zhang, J., Zhang, Z., Miller, W., and Lipman, D. J. (1997). Gapped BLAST and PSI-BLAST: A new generation of protein database search programs. *Nucleic Acids Res.* **25:** 3389–3402.

Anderson, B. L., Boldogh, I., Evangelista, M., Boone, C., Greene, L. A., and Pon, L. A. (1998). The Src homology domain 3 (SH3) of a yeast type I myosin, Myo5p, binds to verprolin and is required for targeting to sites of actin polarization. *J. Cell Biol.* **141:** 1357–1370.

Ausubel, F. M. (1991). "Current Protocols in Molecular Biology," Greene and Wiley–Interscience, New York.

Avraham, K. B., Hasson, T., Sobe, T., Balsara, B., Testa, J. R., Skvorak, A. B., Morton, C. C., Copeland, N. G., and Jenkins, N. A. (1997). Characterization of unconventional MYO6, the human homologue of the gene responsible for deafness in Snell's waltzer mice. *Hum. Mol. Genet.* **6:** 1225–1231.

Avraham, K. B., Hasson, T., Steel, K. P., Kingsley, D. M., Russell, L. B., Mooseker, M. S., Copeland, N. G., and Jenkins, N. A. (1995). The mouse Snell's waltzer deafness gene encodes an unconventional myosin required for structural integrity of inner ear hair cells. *Nat. Genet.* **11:** 369–375.

Baker, J. P., and Titus, M. A. (1997). A family of unconventional myosins from the nematode *Caenorhabditis elegans*. *J. Mol. Biol.* **272:** 523–535.

Baker, J. P., and Titus, M. A. (1998). Myosins: Matching functions with motors. *Curr. Opin. Cell Biol.* **10:** 80–86.

Berger, B., Wilson, D. B., Wolf, E., Tonchev, T., Milla, M., and Kim, P. S. (1995). Predicting coiled coils by use of pairwise residue correlations. *Proc. Natl. Acad. Sci. USA* **92:** 8259–8263.

Burge, C. B., and Karlin, S. (1998). Finding the genes in genomic DNA. *Curr. Opin. Struct. Biol.* **8:** 346–354.

Chen, Z. Y., Hasson, T., Kelley, P. M., Schwender, B. J., Schwartz, M. F., Ramakrishnan, M., Kimberling, W. J., Mooseker, M. S., and Corey, D. P. (1996). Molecular cloning and domain structure of human myosin-VIIa, the gene product defective in Usher syndrome 1B. *Genomics* **36:** 440–448.

Chishti, A. H., Kim, A. C., Marfatia, S. M., Lutchman, M., Hanspal, M., Jindal, H., Liu, S. C., Low, P. S., Rouleau, G. A., Mohandas, N., Chasis, J. A., Conboy, J. G., Gascard, P., Takakuwa, Y., Huang, S. C., Benz, E. J., Jr., Bretscher, A., Fehon, R. G., Gusella, J. F., Ramesh, V., Solomon, F., Marchesi, V. T., Tsukita, S., Hoover, K. B., *et al.* (1998). The FERM domain: A unique module involved in the linkage of cytoplasmic proteins to the membrane. *Trends Biochem. Sci.* **23:** 281–282.

Cope, M. J. T., Whisstock, J., Rayment, I., and Kendrick-Jones, J. (1996). Conservation within the myosin motor domain: Implications for structure and function. *Structure* **4:** 969–987.

Dalgarno, D. C., Botfield, M. C., and Rickles, R. J. (1997). SH3 domains and drug design: Ligands, structure and biological function. *Biopolymers* **43:** 383–400.

DeRosier, D. J., and Tilney, L. G. (1989). The structure of the cuticular plate, an in vivo actin gel. *J. Cell Biol.* **109:** 2853–2867.

Ewing, B., and Green, P. (1998). Base-calling of automated sequencer traces using phred. II. Error probabilities. *Genome Res.* **8:** 186–194.

Ewing, B., Hillier, L., Wendl, M. C., and Green, P. (1998). Base-calling of automated sequencer traces using phred. I. Accuracy assessment. *Genome Res.* **8:** 175–185.

Friedman, T. B., Liang, Y., Weber, J. L., Hinnant, J. T., Barber, T. D., Winata, S., Arhya, I. N., and Asher, J. H., Jr. (1995). A gene for congenital, recessive deafness DFNB3 maps to the pericentromeric region of chromosome 17. *Nat. Genet.* **9:** 86–91.

Garcia, J. A., Yee, A. G., Gillespie, P. G., and Corey, D. P. (1998). Localization of myosin-Ibeta near both ends of tip links in frog saccular hair cells. *J. Neurosci.* **18:** 8637–8647.

Gillespie, P. G., Wagner, M. C., and Hudspeth, A. J. (1993). Identification of a 120 kd hair-bundle myosin located near stereociliary tips. *Neuron* **11:** 581–594.

Gordon, D., Abajian, C., and Green, P. (1998). Consed: A graphical tool for sequence finishing. *Genome Res.* **8:** 195–202.

Hackney, D. D., Levitt, J. D., and Suhan, J. (1992). Kinesin undergoes a 9 S to 6 S conformational transition. *J. Biol. Chem.* **267:** 8696–8701.

Hasson, T., Gillespie, P. G., Garcia, J. A., MacDonald, R. B., Zhao, Y., Yee, A. G., Mooseker, M. S., and Corey, D. P. (1997). Unconventional myosins in inner-ear sensory epithelia. *J. Cell Biol.* **137:** 1287–1307.

Hasson, T., Heintzelman, M. B., Santos-Sacchi, J., Corey, D. P., and Mooseker, M. S. (1995). Expression in cochlea and retina of myosin VIIa, the gene product defective in Usher syndrome type 1B. *Proc. Natl. Acad. Sci. USA* **92:** 9815–9819.

Houdusse, A., Silver, M., and Cohen, C. (1996). A model of Ca(2+)-free calmodulin binding to unconventional myosins reveals how calmodulin acts as a regulatory switch. *Structure* **4:** 1475–1490.

Hudspeth, A. J. (1992). Hair-bundle mechanics and a model for mechanoelectrical transduction by hair cells. *Soc. Gen. Physiol. Ser.* **47:** 357–370.

Hudspeth, A. J., and Gillespie, P. G. (1994). Pulling springs to tune transduction: Adaptation by hair cells. *Neuron* **12:** 1–9.

Kapeller, R., Prasad, K. V., Janssen, O., Hou, W., Schaffhausen, B. S., Rudd, C. E., and Cantley, L. C. (1994). Identification of two SH3-binding motifs in the regulatory subunit of phosphatidylinositol 3-kinase. *J. Biol. Chem.* **269:** 1927—1933.

Kelley, C. A., Takahashi, M., Yu, J. H., and Adelstein, R. S. (1993). An insert of seven amino acids confers functional differences between smooth muscle myosins from the intestines and vasculature. *J. Biol. Chem.* **268:** 12848–12854.

Kozak, M. (1996). Interpreting cDNA sequences: Some insights from studies on translation. *Mamm. Genome* **7:** 563–574.

Liang, J., Chen, J. K., Schreiber, S. T., and Clardy, J. (1996). Crystal structure of P13K SH3 domain at 20 angstroms resolution. *J. Mol. Biol.* **257:** 632–643.

Liang, Y., Wang, A., Probst, F. J., Arhya, I. N., Barber, T. D., Chen, K. S., Deshmukh, D., Dolan, D. F., Hinnant, J. T., Carter, L. E., Jain, P. K., Lalwani, A. K., Li, X. C., Lupski, J. R., Moeljopawiro, S., Morell, R., Negrini, C., Wilcox, E. R., Winata, S., Camper, S. A., and Friedman, T. B. (1998). Genetic mapping refines DFNB3 to 17p11.2, suggests multiple alleles of DFNB3, and supports homology to the mouse model shaker 2. *Am. J. Hum. Genet.* **62:** 904–915.

Liu, X. Z., Walsh, J., Mburu, P., Kendrick-Jones, J., Cope, M. J., Steel, K. P., and Brown, S. D. (1997a). Mutations in the myosin VIIA gene cause non-syndromic recessive deafness. *Nat. Genet.* **16:** 188–190.

Liu, X. Z., Walsh, J., Tamagawa, Y., Kitamura, K., Nishizawa, M., Steel, K. P., and Brown, S. D. (1997b). Autosomal dominant non-syndromic deafness caused by a mutation in the myosin VIIA gene. *Nat. Genet.* **17:** 268–269.

Lloyd, R. V., Jin, L., Qian, X., Scheithauer, B. W., Young, W. F., Jr., and Davis, D. H. (1995). Analysis of the chromogranin A post-translational cleavage product pancreastatin and the prohormone convertases PC2 and PC3 in normal and neoplastic human pituitaries. *Am. J. Pathol.* **146:** 1188–1198.

Mayer, B. J., and Gupta, R. (1998). Functions of SH2 and SH3 domains. *Curr. Top. Microbiol. Immunol.* **228:** 1–22.

Mburu, P., Liu, X. Z., Walsh, J., Saw, D., Jr., Cope, M. J., Gibson, F., Kendrick-Jones, J., Steel, K. P., and Brown, S. D. (1997). Mutation analysis of the mouse myosin VIIA deafness gene. *Genes Funct.* **1:** 191–203.

Mermall, V., Post, P. L., and Mooseker, M. S. (1998). Unconventional myosins in cell movement, membrane traffic, and signal transduction. *Science* **279:** 527–533.

Montell, C., and Rubin, G. M. (1988). The Drosophila ninaC locus encodes two photoreceptor cell specific proteins with domains homologous to protein kinases and the myosin heavy chain head. *Cell* **52:** 757–772.

Mooseker, M. S., and Cheney, R. E. (1995). Unconventional myosins. *Annu. Rev. Cell Dev. Biol.* **11:** 633–675.

Musacchio, A., Gibson, T., Lehto, V. P., and Saraste, M. (1992). SH3—An abundant protein domain in search of a function. *FEBS Lett.* **307:** 55–61.

Olney, J. J., Sellers, J. R., and Cremo, C. R. (1996). Structure and function of the 10 S conformation of smooth muscle myosin. *J. Biol. Chem.* **271:** 20375–20384.

Porter, J. A., and Montell, C. (1993). Distinct roles of the *Drosophila* ninaC kinase and myosin domains revealed by systematic mutagenesis. *J. Cell Biol.* **122:** 601–612.

Probst, F. J., Fridell, R. A., Raphael, Y., Saunders, T. L., Wang, A., Liang, Y., Morell, R. J., Touchman, J. W., Lyons, R. H., Noben-Trauth, K., Friedman, T. B., and Camper, S. A. (1998). Correction of deafness in shaker 2 mice by an unconventional myosin in a BAC transgene. *Science* **280:** 1444–1447.

Qian, X., Jin, L., Grande, J. P., and Lloyd, R. V. (1996). Transforming growth factor-beta and p27 expression in pituitary cells. *Endocrinology* **137:** 3051–3060.

Rayment, I., Rypniewski, W. R., Schmidt-Base, K., Smith, R., Tomchick, D. R., Benning, M. M., Winkelmann, D. A., Wesenberg, G., and Holden, H. M. (1993). Three-dimensional structure of myosin subfragment-1: A molecular motor. *Science* **261:** 50–58.

Ressler, K. J., Sullivan, S. L., and Buck, L. B. (1994). Information coding in the olfactory system: Evidence for a stereotyped and highly organized epitope map in the olfactory bulb. *Cell* **79:** 1245–1255.

Sassoon, D. A., Garner, I., and Buckingham, M. (1988). Transcripts of alpha-cardiac and alpha-skeletal actins are early markers for myogenesis in the mouse embryo. *Development* **104:** 155–164.

Schenker, T., Lach, C., Kessler, B., Calderara, S., and Trueb, B. (1994). A novel GTP-binding protein which is selectively repressed in SV40 transformed fibroblasts. *J. Biol. Chem.* **269:** 25447–25453.

Schwartz, S., Miller, W., Yang, C. M., and Hardison, R. C. (1991). Software tools for analyzing pairwise alignments of long sequences. *Nucleic Acids Res.* **19:** 4663–4667.

Sellers, J. R. (1999). "Myosin," Oxford Univ. Press, London.

Steyger, P. S., Gillespie, P. G., and Baird, R. A. (1998). Myosin Ibeta is located at tip link anchors in vestibular hair bundles. *J. Neurosci.* **18:** 4603–4615.

Trybus, K. M., Huiatt, T. W., and Lowey, S. (1982). A bent monomeric conformation of myosin from smooth muscle. *Proc. Natl. Acad. Sci. USA* **79:** 6151–6155.

Wakabayashi, Y., Takahashi, Y., Kikkawa, Y., Okano, H., Mishima, Y., Ushiki, T., Yonekawa, H., and Kominami, R. (1998). A novel type of myosin encoded by the mouse deafness gene shaker 2. *Biochem. Biophys. Res. Commun.* **248:** 655–659.

Wang, A., Liang, Y., Fridell, R. A., Probst, F. J., Wilcox, E. R., Touchman, J. W., Morton, C. C., Morell, R. J., Noben-Trauth, K., Camper, S. A., and Friedman, T. B. (1998). Association of unconventional myosin MYO15 mutations with human nonsyndromic deafness DFNB3. *Science* **280:** 1447–1451.

Weil, D., Blanchard, S., Kaplan, J., Guilford, P., Gibson, F., Walsh, J., Mburu, P., Varela, A., Levilliers, J., Weston, M. D., *et al.* (1995). Defective myosin VIIA gene responsible for Usher syndrome type 1B. *Nature* **374:** 60–61.

Weil, D., Kussel, P., Blanchard, S., Levy, G., Levi-Acobas, F., Drira, M., Ayadi, H., and Petit, C. (1997). The autosomal recessive isolated deafness, DFNB2, and the Usher 1B syndrome are allelic defects of the myosin-VIIA gene. *Nat. Genet.* **16:** 191–193.

Weil, D., Levy, G., Sahly, I., Levi-Acobas, F., Blanchard, S., El-Amraoui, A., Crozet, F., Philippe, H., Abitbol, M., and Petit, C. (1996). Human myosin VIIA responsible for the Usher 1B syndrome: A predicted membrane-associated motor protein expressed in developing sensory epithelia. *Proc. Natl. Acad. Sci. USA* **93:** 3232–3237.

Wilson, R. K., and Mardis, E. R. (1997). Shotgun sequencing. *In* "Analyzing DNA" (B. Birren, E. D. Green, S. Klapholz, R. M. Myers, and J. Roskams, Eds.), pp. 397–454, Cold Spring Harbor Laboratory Press, Cold Spring Harbor, NY.

Xu, P., Mitchelhill, K. I., Kobe, B., Kemp, B. E., and Zot, H. G. (1997). The myosin-I-binding protein Acan125 binds the SH3 domain and belongs to the superfamily of leucine-rich repeat proteins. *Proc. Natl. Acad. Sci. USA* **94:** 3685–3690.